



Heriot-Watt University
Research Gateway

Single shot i-Toffoli gate in dispersively coupled superconducting qubits

Citation for published version:

Baker, AJ, Huber, GBP, Glaser, NJ, Roy, F, Tsitsilin, I, Filipp, S & Hartmann, MJ 2022, 'Single shot i-Toffoli gate in dispersively coupled superconducting qubits', *Applied Physics Letters*, vol. 120, no. 5, 054002.
<https://doi.org/10.1063/5.0077443>

Digital Object Identifier (DOI):

[10.1063/5.0077443](https://doi.org/10.1063/5.0077443)

Link:

[Link to publication record in Heriot-Watt Research Portal](#)

Document Version:

Publisher's PDF, also known as Version of record

Published In:

Applied Physics Letters

Publisher Rights Statement:

This article may be downloaded for personal use only. Any other use requires prior permission of the author and AIP Publishing. This article appeared in Appl. Phys. Lett. 120, 054002 (2022) and may be found at <https://doi.org/10.1063/5.0077443>

General rights

Copyright for the publications made accessible via Heriot-Watt Research Portal is retained by the author(s) and / or other copyright owners and it is a condition of accessing these publications that users recognise and abide by the legal requirements associated with these rights.

Take down policy

Heriot-Watt University has made every reasonable effort to ensure that the content in Heriot-Watt Research Portal complies with UK legislation. If you believe that the public display of this file breaches copyright please contact open.access@hw.ac.uk providing details, and we will remove access to the work immediately and investigate your claim.

Single shot i-Toffoli gate in dispersively coupled superconducting qubits ^{EP}

Cite as: Appl. Phys. Lett. **120**, 054002 (2022); <https://doi.org/10.1063/5.0077443>

Submitted: 02 November 2021 • Accepted: 06 January 2022 • Published Online: 03 February 2022

 Aneirin J. Baker, Gerhard B. P. Huber, Niklas J. Glaser, et al.

COLLECTIONS

Paper published as part of the special topic on [Emerging Qubit Systems - Novel Materials, Encodings and Architectures](#)

 This paper was selected as an Editor's Pick



View Online



Export Citation



CrossMark

ARTICLES YOU MAY BE INTERESTED IN

[In situ Raman spectroscopy across superconducting transition of liquid-gated MoS₂](#)

Applied Physics Letters **120**, 053106 (2022); <https://doi.org/10.1063/5.0077464>

[Nanometer-thin L₁O-MnAl film with B₂-CoAl underlayer for high-speed and high-density STT-MRAM: Structure and magnetic properties](#)

Applied Physics Letters **120**, 052404 (2022); <https://doi.org/10.1063/5.0077874>

[Epitaxial growth and thermoelectric properties of Mg₃Bi₂ thin films deposited by magnetron sputtering](#)

Applied Physics Letters **120**, 051901 (2022); <https://doi.org/10.1063/5.0074419>



Timing is everything.
Now it's automatic.

A new synchronous source measure system for electrical measurements of materials and devices

 **Lake Shore**
CRYOTRONICS

[Learn more](#)

Single shot i-Toffoli gate in dispersively coupled superconducting qubits

Cite as: Appl. Phys. Lett. **120**, 054002 (2022); doi: [10.1063/5.0077443](https://doi.org/10.1063/5.0077443)

Submitted: 2 November 2021 · Accepted: 6 January 2022 ·

Published Online: 3 February 2022






View Online



Export Citation



CrossMark

Aneirin J. Baker,^{1,a)}  Gerhard B. P. Huber,^{2,3} Niklas J. Glaser,^{2,3} Federico Roy,^{3,4} Ivan Tsitsilin,^{2,3} Stefan Filipp,^{2,3,5}  and Michael J. Hartmann⁶ 

AFFILIATIONS

¹SUPA, Institute of Photonics and Quantum Sciences, Heriot-Watt University, Edinburgh EH14 4AS, United Kingdom

²Department of Physics, Technical University of Munich, 85748 Garching, Germany

³Walther-Meißner-Institut, Bayerische Akademie der Wissenschaften, 85748 Garching, Germany

⁴Theoretical Physics, Saarland University, 66123 Saarbrücken, Germany

⁵Munich Center for Quantum Science and Technology (MSQCT), Schellingstraße 4, 80799 München, Germany

⁶Department of Physics, Friedrich-Alexander University Erlangen-Nürnberg (FAU), Erlangen, Germany and Max Planck Institute for the Science of Light, Erlangen, Germany

Note: This paper is part of the APL Special Collection on Emerging Qubit Systems - Novel Materials, Encodings and Architectures.

a) Author to whom correspondence should be addressed: ajb17@hw.ac.uk

ABSTRACT

Quantum algorithms often benefit from the ability to execute multi-qubit (>2) gates. To date, such multi-qubit gates are typically decomposed into single- and two-qubit gates, particularly in superconducting qubit architectures. The ability to perform multi-qubit operations in a single step could vastly improve the fidelity and execution time of many algorithms. Here, we propose a single shot method for executing an i-Toffoli gate, a three-qubit gate with two control and one target qubit, using currently existing superconducting hardware. We show numerical evidence for a process fidelity over 99.5% and a gate time of 450 ns for superconducting qubits interacting via tunable couplers. Our method can straight forwardly be extended to implement gates with more than two control qubits at similar fidelities.

Published under an exclusive license by AIP Publishing. <https://doi.org/10.1063/5.0077443>

The implementation of gate based quantum algorithms has made groundbreaking advances in recent years, particularly in superconducting circuit architectures.¹ Quantum computing is, thus, entering the so-called Noisy Intermediate Scale Quantum Computer (NISQ) era,² where devices are getting powerful enough to challenge classical computing power but fall short of allowing for implementation of quantum error correction. Despite this remarkable progress, achievable gate fidelities still limit the number of gates that can be executed in a circuit and, thus, limit applications.

A possible step forward could be to replace multi-qubit gate decomposition's by a single multi-qubit gate. The Toffoli or controlled-controlled Not (CCX) gate, for example, requires at least six CNOT gates³ and other single qubit gates in its decomposition. This severely affects the fidelity and gate time of such higher order gates. For a single step multi-qubit gate to be helpful, it needs to be executed with better fidelity and shorter execution time than the equivalent decomposition. Particularly in superconducting circuits, the attention has so far been focused on the latter since the qubits

typically only interact with their direct neighbors. These higher order gates are, however, crucial ingredients of more complex algorithms, such as Quantum Error Correction,⁴ Grover's Search Algorithm,⁵ and algorithms for Quantum Chemistry.^{6,7} The Toffoli gate (which is required for designing quantum analogues of classical algorithms) is a prime example of a higher order gate that would benefit from a single shot implementation.

Here, we propose a mechanism for performing higher order gates on current superconducting hardware and architectures, using a recent idea⁸ adapted for a more viable implementation in readily existing hardware. We utilize the ZZ couplings that can be engineered with capacitive or tunable couplers in superconducting circuits (SCCs) via dispersive shifts in the qubit transition frequencies.^{9–11} We note here that ZZ couplings that could be generated by the nonlinear interaction originating from directly connecting the qubits via a Josephson junction^{8,10} do not lead to scalable lattices since they generate closed loops, where flux quantization makes the device highly sensitive to flux noise.

In our system, we consider dispersive ZZ interactions that shift the transition frequencies of the qubits conditioned on the states of the qubits that they interact with. Selecting one qubit as the target qubit, we can, thus, apply a single qubit drive on this $|0\rangle \leftrightarrow |1\rangle$ transition, which is dispersively shifted by the ZZ interactions. This drive executes a high-fidelity flip of this target qubit, if and only if the two remaining qubits are in the $|1\rangle$ states. For our system this results in the $|101\rangle \leftrightarrow |111\rangle$ transition, where the first and third qubits are the controls and the second qubit the target qubit. All other input states remain invariant. As we show below, this scheme, thus, leads to the implementation of an i-Toffoli gate, which has a matrix representation

$$U_{i\text{-Toffoli}} = \begin{pmatrix} 1 & 0 & 0 & 0 & 0 & 0 & 0 & 0 \\ 0 & 1 & 0 & 0 & 0 & 0 & 0 & 0 \\ 0 & 0 & 1 & 0 & 0 & 0 & 0 & 0 \\ 0 & 0 & 0 & 1 & 0 & 0 & 0 & 0 \\ 0 & 0 & 0 & 0 & 1 & 0 & 0 & 0 \\ 0 & 0 & 0 & 0 & 0 & 0 & 0 & -i \\ 0 & 0 & 0 & 0 & 0 & 0 & 1 & 0 \\ 0 & 0 & 0 & 0 & 0 & -i & 0 & 0 \end{pmatrix}$$

in the computational basis.

For this scheme to work with high-fidelity, the dispersively shifted transitions need to be individually addressable, which requires the drive amplitude to be smaller than the shifts.¹² The gate time is, therefore, only dependent on the strength of this drive. These dispersive shifts can be turned on and off using a tunable SQUID coupler, meaning that a high level of control can be exerted over this system. Such tunable couplers are essential ingredients of today's most advanced architectures.^{1,13}

Previous realizations of a Toffoli gate have had a gate fidelity of 68.5% with a gate time of 50 ns (Ref. 14) using a technique of hiding the target qubit excitations in higher energy states and reached 87% process fidelity in more recent realizations.¹⁵ A very recent implementation of an i-Toffoli via cross-resonance driving of capacitively coupled transmon qubits reached gate time of 350 ns and 98% process fidelity.¹⁶ This approach uses cross resonance drives on all three fixed frequency qubits.

In contrast, our proposal works with transmon qubits coupled via tunable couplers and achieves a process fidelity of over 99.5% for a gate time of 450 ns with the application of a single microwave pulse on the center qubit. Since we consider the same types of qubits and coupling circuits as implemented in the hardware of most leading developers,^{1,13,17–19} our approach adds further versatility to the possible gates that current quantum chips can run.

One of its most important features is that it can be generalized to more than two control qubits, e.g., to CCCX gates, without noticeable loss of fidelity. To this end, the frequency of the drive applied to the target qubit needs to be chosen such that it only picks out the specific CCCX transition we require. For current hardware with qubits on a regular 2d grid, this would, for example, allow us to execute not gates controlled by four qubits (as similarly explored with qubits and resonators²⁰). Another generalization of this system is to use more than one drive. This would allow the system to detect qubit cluster parity,²¹ which is crucial for quantum error correction.

We consider three qubits coupled via two tunable couplers, where the qubits are capacitively coupled to the tunable couplers, providing a tunable interaction^{22,23} between the target and control qubits as demonstrated in Refs. 17 and 24–26, see Fig. 1 for a circuit diagram.

By adjusting the coupler transition frequencies with external fluxes, we can tune the couplings^{27,28} giving versatile control over the interactions of this system. We use transmon qubits²⁹ and capacitively shunted dc-SQUIDS as tunable couplers. After quantization of the circuit and dropping counter rotating terms (see the [supplementary material](#) for full derivation), we obtain the Hamiltonian

$$H = \sum_{i=1}^3 \left(\omega_i q_i^\dagger q_i + \frac{\alpha_i}{2} q_i^\dagger q_i^\dagger q_i q_i \right) + \sum_{j=1}^2 \left(\omega_{cj} c_j^\dagger c_j + \frac{\alpha_{cj}}{2} c_j^\dagger c_j^\dagger c_j c_j \right) - \sum_{n < m=1}^3 g_{nm} (q_n^\dagger q_m + q_m^\dagger q_n) - \sum_{k=1}^2 g_{k,c1} (c_k^\dagger q_1 + q_1^\dagger c_k) - \sum_{l=2}^3 g_{l,c2} (c_l^\dagger q_2 + q_2^\dagger c_l) + \Omega(t) (q_2 + q_2^\dagger), \quad (1)$$

where q_i (c_i) represent the annihilation operators for the qubits (couplers) and ω_i/α_i (ω_{cj}/α_{cj}) are the qubit (coupler) transition frequencies and anharmonicities, respectively. The external voltage drive applied to the target qubit is denoted by $\Omega(t)$, g_{nm} denotes the coupling between qubit n and m (the exact form can be found in the [supplementary material](#)), and $g_{i,cj}$ describes the coupling between the i -th qubit and the j -th coupler. We choose capacitances such that the coupling between the qubits is much smaller than the qubit-coupler coupling. We detune the coupler and qubits by >1 GHz to ensure that the counter rotating terms do not contribute.²⁵ In this dispersive regime (i.e., $\frac{g_{i,cj}}{\omega_i - \omega_{cj}} \ll 1$), we can eliminate the coupler using a Schrieffer-Wolff (SW) transformation,³⁰ $H \rightarrow \tilde{H} = e^{iS} H e^{-iS}$, where $S = \sum_{i=1}^2 \frac{g_{i,c1}}{\omega_i - \omega_{c1}} (q_i^\dagger c_1 - q_i c_1^\dagger) + \sum_{j=2}^3 \frac{g_{j,c2}}{\omega_j - \omega_{c2}} (q_j^\dagger c_2 - q_j c_2^\dagger)$. Keeping terms up to the second order in this expansion, we decouple the qubits from the couplers such that we are only left with qubit-qubit couplings described by the Hamiltonian

$$\tilde{H} = H_{0,q} + H_{qq} + H_d, \quad (2)$$

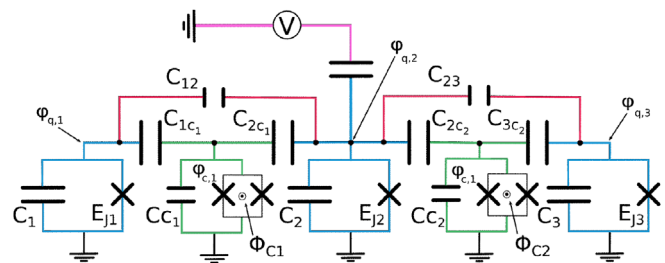


FIG. 1. Circuit diagram of our system; here, the blue circuits indicate the qubit nodes (described by $\varphi_{q,i}$). Each qubit has a capacitance of C_i and a Josephson Energy of $E_{J,i}$. The green circuits indicate the tunable couplers (described by $\varphi_{c,i}$). The tunable couplers have capacitance $C_{c,i}$, Josephson Energy of $E_{J,c,i}$, and they are driven by an external flux $\Phi_{c,i}$, which tunes their frequency. The second qubit is driven by an external voltage (denoted in pink here), which executes the CCX interaction. The qubits are coupled to one another via a small capacitance C_{ij} (red circuits), and the qubits and tunable couplers are each coupled via a capacitance $C_{i,cj}$.

where ($\hbar = 1$)

$$\begin{aligned} H_{0,q} &= \sum_{j=1}^3 \tilde{\omega}_j q_j^\dagger q_j + \frac{\tilde{\alpha}_j}{2} q_j^\dagger q_j^\dagger q_j q_j, \\ H_{qq} &= \sum_{n < m=1}^3 \tilde{g}_{nm} (q_n q_m^\dagger + q_n^\dagger q_m), \\ H_d &= \Omega(t)(q_2 + q_2^\dagger). \end{aligned} \quad (3)$$

Here, $\tilde{\omega}_n$, $\tilde{\alpha}_n$, and \tilde{g}_{nm} are shifted frequencies, nonlinearities, and couplings (see the [supplementary material](#) for the explicit expressions). We have dropped the counter rotating terms and assumed that the coupler always remains in the ground state. The latter allows us to drop the terms describing the coupler as it is no longer coupled to the qubits.

Following the procedure outlined in Ref. 31, we use perturbation theory to calculate the corrections to the eigenenergies of $H_{0,q}$ due to the interaction term $V = H_{qq}$. We use these to calculate the dispersive shifts χ_{nm} , where n and m denote the qubits that the shift applies to,

$$\begin{aligned} \chi_{12} &= E_{|110\rangle} - E_{|100\rangle} - E_{|010\rangle} + E_{|000\rangle}, \\ \chi_{13} &= E_{|101\rangle} - E_{|100\rangle} - E_{|001\rangle} + E_{|000\rangle}, \\ \chi_{23} &= E_{|011\rangle} - E_{|010\rangle} - E_{|001\rangle} + E_{|000\rangle}, \end{aligned} \quad (4)$$

and the total shift on the $|111\rangle$ state,

$$\chi_{123} = E_{|111\rangle} - E_{|100\rangle} - E_{|010\rangle} - E_{|001\rangle} + 2E_{|000\rangle}, \quad (5)$$

up to the second order. Here, $E_{|n\rangle}$ denotes the energy of the state $|n\rangle$, including corrections up to the second order in H_{qq} . We note that χ_{123} contains all possible shifts on the $|111\rangle$ state, and this will include both controlled phase (CPhase) and controlled controlled phase (CCPhase) shifts (see the [supplementary material](#) for discussion of CCPhase), which emerge because of the finite nonlinearity of transmon qubits, see Eq. (7). The dispersive shifts can be expanded in orders of perturbation theory $\chi^{(n)}$,

$$\chi_m = \chi_m^{(1)} + \chi_m^{(2)} + \dots, \quad (6)$$

where $m \in \{12, 13, 23, 123\}$. We note that all first order terms vanish, $\chi_m^{(1)} = 0$, as the interaction term V is off diagonal. To the second order, we obtain the following shifts:

$$\begin{aligned} \chi_{ij}^{(2)} &= -\frac{2\tilde{g}_{ij}^2}{\tilde{\alpha}_i + \tilde{\Delta}_{ij}} - \frac{2\tilde{g}_{ij}^2}{\tilde{\alpha}_j + \tilde{\Delta}_{ij}} + \frac{2\tilde{g}_{ij}^2}{\tilde{\alpha}_i + \tilde{\Sigma}_{ij}} + \frac{2\tilde{g}_{ij}^2}{\tilde{\alpha}_j + \tilde{\Sigma}_{ij}} - \frac{4\tilde{g}_{ij}^2}{\tilde{\alpha}_i + \tilde{\alpha}_j + \tilde{\Sigma}_{ij}}, \\ \chi_{123}^{(2)} &= \chi_{12}^{(2)} + \chi_{23}^{(2)} + \chi_{13}^{(2)}, \end{aligned} \quad (7)$$

where we have introduced the notation $\tilde{\Delta}_{ij} = \tilde{\omega}_i - \tilde{\omega}_j$ and $\tilde{\Sigma}_{ij} = \tilde{\omega}_i + \tilde{\omega}_j$. In a frame, where each qubit rotates at its transition frequency (including second order perturbative corrections) and neglecting χ_{13} and neglecting χ_{13} and all shifts greater than third order in perturbation theory by choosing parameters such that these perturbations are highly suppressed. We, thus, arrive at the Hamiltonian

$$\begin{aligned} \tilde{H}_{2-Lvl} &= \chi_{12}^{(2)}(|110\rangle\langle 110| + |111\rangle\langle 111|) \\ &+ \chi_{23}^{(2)}(|011\rangle\langle 011| + |111\rangle\langle 111|) + H_d, \end{aligned} \quad (8)$$

in a two level approximation.

The dispersive shifts can be thought of as shifts in the qubit transition frequency dependent on the state of the other qubits. For suitable drive frequencies, this allows us to individually address specific transitions of the three qubit system as each excited qubit adds a contribution to the dispersive shift of the target qubit. This results in the $|110\rangle$, $|011\rangle$, and $|111\rangle$ states being shifted by χ_{12} , χ_{23} , and $\chi_{12} + \chi_{23}$, respectively. In our case, we wish to address the $|101\rangle \leftrightarrow |111\rangle$ transition, which will be shifted by $\chi_{12} + \chi_{23}$ by the external drive to produce an i-Toffoli gate. The level diagram and suitable control pulses are sketched in Fig. 2.

Our approach relies on ZZ interactions that cause the dispersive shifts as an essential ingredient. These dispersive shifts induce conditional phase accumulation on specific states, which can be described by the unitary $U_{\text{phase}} = \text{diag}[1, 1, 1, e^{i\chi_{23}t}, 1, 1, e^{i(\chi_{12} + \chi_{23})t}]$. These conditional phases correspond to CPhase gates that are included in our three qubit gate. One can either work with this generalized Toffoli gate or apply simple strategies to eliminate the contributions of conditional phase gates. We can cancel the accumulated phase (χ_{ij}) by applying CPhase gates after the Toffoli gate has been executed. After having corrected for the phases discussed above and removing any single qubit phases, we are left with a factor of $-i$ multiplying the flipped states ($|111\rangle$ and $|101\rangle$).⁸ If needed, this factor could be removed via the inclusion of an ancilla qubit.⁸ We want to add that Toffoli gates with modified phases have been found to be useful in certain quantum algorithms.³²

Given the above discussion, we can determine the unitary that we obtain if all employed approximations work perfectly. We take into consideration the accumulated phases discussed above along with the factor of $-i$ caused by the drive only being resonant with the subspace $\{|101\rangle, |111\rangle\}$, which we are, thus, not able to compensate for with a virtual Z gate. Denoting \tilde{U} the unitary that results from a perturbation free evolution as generated by \tilde{H}_{2-Lvl} as in Eq. (8) and using U_{phase}^\dagger as a perfect phase correcting unitary, which corrects for the accumulated phases, we find

$$U_{i\text{-Toffoli}} = U_{\text{phase}}^\dagger \tilde{U}, \quad (9)$$

where $U_{i\text{-Toffoli}}$ is defined in Eq. (1).

We numerically simulated the dynamics generated by the Hamiltonian \tilde{H} of Eq. (2) using QUTIP³³ and the q-optimize package.³⁴ We truncate the qubit subspace to only include three energy levels. By performing sweeps over realistic parameter ranges,

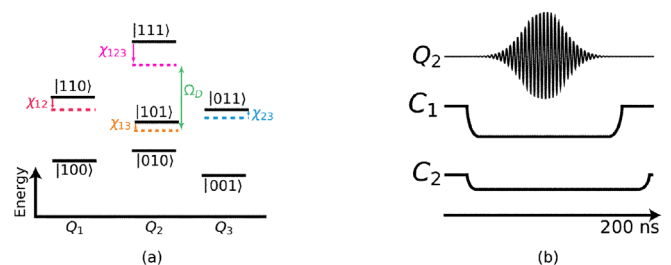


FIG. 2. (a) Energy level diagram detailing the dispersive shifts and couplings within the system. Also showing the applied drive. (b) Suggested pulse schemes for an experimental realization. C_1 and C_2 show the biases applied to the couplers bringing them to the needed frequency to cause the dispersive shifts and Q_2 showing the drive pulse applied to qubit 2.

we identified suitable parameters for the circuit and then used the q-optimize package to optimize the drive pulse. We applied DRAG (Derivative Removal by Adiabatic Gate)³⁵ to shape the Gaussian pulses such that states outside the computational subspace are not excited despite the presence of the dispersive shifts.

Denoting by U_{sim} as the unitary that results from the simulated dynamics generated by \hat{H} , we quantify the fidelity of the gate by comparing $U_{phase}^\dagger U_{sim}$ and $U_{i-Toffoli}$. In terms of process fidelity, as measured by the entanglement fidelity $F_p(U_1, U_2) = |\text{Tr}(U_1^\dagger U_2)|/d$ ($d=8$ being the dimension of the Hilbert space), our scheme reaches $F_p(U_{i-Toffoli}, U_{phase}^\dagger U_{sim}) \geq 99.5\%$ for the parameters stated below.

We choose qubit frequencies $\tilde{\omega}_1/2\pi = 4.965$, $\tilde{\omega}_2/2\pi = 5.12$, and $\tilde{\omega}_3/2\pi = 4.825$ GHz, to maximize fidelity and ensure that our approximations are highly accurate (leading terms of the neglected perturbations are sufficiently small). The peak drive amplitude of the considered Gaussian pulse was $|\Omega|/2\pi = 2.1$ MHz. The corresponding simulation results are shown in Fig. 3, see the figure caption for the remaining parameters.

The conditions, which limit the achievable process fidelity in our scheme, are: (i) The gate needs to be executed much quicker than the decoherence time of the qubits, where a quicker gate requires a larger drive. (ii) To avoid excitations of higher energy states, the drive needs to remain in the weak driving regime, where increasing the drive amplitude ($|\Omega(t)|$) would require a similar increase in the dispersive shifts χ_{12} and χ_{23} . The latter could be achieved by decreasing the detuning Δ . (iii) The detuning Δ , however, needs to remain large enough to keep the device in the dispersive regime. (iv) The pulse $\Omega(t)$ needs to be such that non-computational states remain unoccupied. (v) The parameters need to be chosen such that the unwanted interactions leading to CPhase action on the $|111\rangle$ state are minimized.

To further analyze the sources of error in our scheme, we note that there are tunable couplers only between neighboring qubits.

Hence, only the phases due to χ_{12} and χ_{23} can be corrected for by CPhase gates, and the dispersive shifts χ_{13} and χ_{123} will cause errors by generating unitary transformations $U_{\chi_{13}}$ and $U_{\chi_{123}}$. From the resulting errors $1 - F_p(U_{i-Toffoli}, U_\alpha U_{i-Toffoli})$ for $\alpha = \chi_{13}(\chi_{123})$, we estimate that they reduce the fidelity by $<0.025\%$ ($<0.004\%$). Our simulations also reveal that unintended leakage to other states leads to unwanted occupations of 0.3% for states in and 0.02% for states outside the computational subspace. The remaining 0.1% of error probability is found to disappear in the limit of large gate time (smaller drive amplitude); thus, we ascribe this error to the drive weakly coupling to states with a resonant frequency close to the drive frequency. This source of error would also be reduced for larger dispersive shifts.

As the gate is executed in less than 1% of the T_1 and T_2 times of modern transmon qubits, dissipation processes will only insignificantly lower the fidelity found in our unitary simulations, e.g., by $\sim 0.5\%$ for $T_1 \sim T_2 \sim 75\mu\text{s}$. Moreover, the CPhase gates employed to correct for phases due to χ_{12} and χ_{23} will have finite fidelities. Assuming 99.5% fidelities for these gates, the overall fidelity for the i-Toffoli process will be reduced by a factor 0.99. Taking all these reductions into account, we estimate the fidelity of the process to be $\sim 98\%$.

The approach to a single shot Toffoli gate that we present here can be modified and enhanced in multiple ways. First, it can also be implemented in a circuit without tunable couplers, e.g., where frequency tunable qubits are capacitively coupled. The absence of tunable couplers would mean a stronger coupling between the qubits, and since the dispersive shift is proportional to the square of this coupling strength, it would lead to a larger shift in qubit transition frequencies, allowing for larger drives and, thus, even faster gate times.

For the simple circuit discussed here, the roles of target and control qubits are not interchangeable. Yet for qubits arranged in a triangle, with tunable couplers between each pair of neighbors, each qubit can take the role of the target qubit. Importantly, in a lattice, where

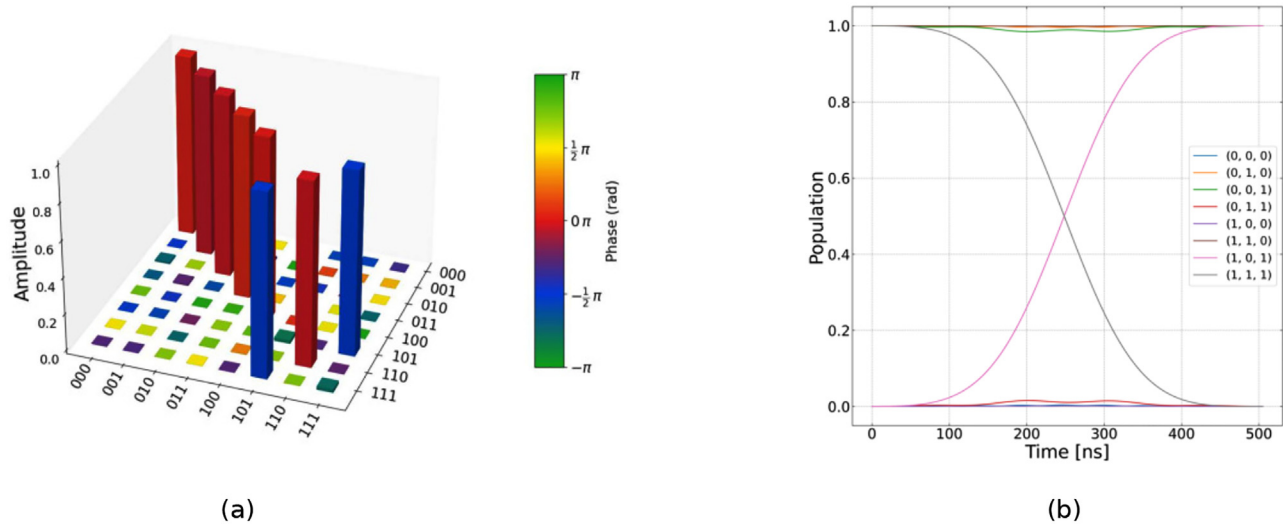


FIG. 3. (a) Absolute values of the matrix elements of $U_{phase}^\dagger U_{sim}$ for our scheme, showing $\geq 99.5\%$ process fidelity. Here, the evolved unitary has been multiplied by a correcting phase unitary to simulate a perfect phase correction process. As a consequence, all phases have returned close to 0. One sees, that the states $|101\rangle$ and $|111\rangle$ are fully swapped, with an added phase of $-\pi/2$, making the gate an i-Toffoli gate. The system parameters (in natural frequency units) used are: qubit frequencies of $\tilde{\omega}_1/2\pi = 4.965$, $\tilde{\omega}_2/2\pi = 5.12$, and $\tilde{\omega}_3/2\pi = 4.825$ GHz. Anharmonicities of $\tilde{\alpha}_1/2\pi = \tilde{\alpha}_3/2\pi = -330$, $\tilde{\alpha}_2/2\pi = -240$ MHz and qubit-qubit coupling strengths of $\tilde{g}_{12}/2\pi = 15.4$, $\tilde{g}_{23}/2\pi = 29.2$, and $\tilde{g}_{13}/2\pi = 2.2$ MHz. The peak drive amplitude was $|\Omega|/2\pi = 2.1$ MHz. The phases of this simulation were corrected against the idle phases simulated using the same parameters. (b) Population transfer in the target qubit, the legend on the right-hand side depicts the initial state.

each qubit has four direct neighbors, as required for surface code realizations, any two of the four neighboring qubits can take the role of control qubits. This could also be achieved by connecting all the qubits to a central tunable coupler,^{36,37} this would allow for tunability of all the couplings via modification of the coupler frequency.

Further extensions of this system can be envisaged by adding more qubits to the circuit, thus allowing us to execute higher order Toffoli gates (Multi-Controlled-Not-Gates), such as, for example, a CCCX gate. As with the standard Toffoli gate, higher order Toffoli gates can be decomposed into single- and two-qubit gates. The number of elementary gates in such expansions, however, scales exponentially with the number of control qubits involved³⁸ and, in some cases, can require many more ancilla qubits.³⁹ The realization of single-shot higher order controlled NOT gates following our scheme would circumvent this problem and allow the use of these gates without modification of existing hardware. These higher order gates have uses in quantum information algorithms [4], quantum error correction,^{4,20,40} and quantum annealing.⁴¹ Since current decomposition's of higher order gates require 2^{n-1} controlled gates (where n is the number of control qubits),³⁹ the fidelity of such decomposed operations would be significantly lower than the single shot implementation, which we propose here.

In summary, we have presented a proposal for a single step Toffoli gate using dispersive shifts. We have numerically simulated the system and find that the achievable process fidelity and gate time are significantly better than most current implementations and comparable to the latest results within superconducting circuits. The proposed implementation uses existing superconducting devices and is, thus, straight-forward to implement in available hardware. The approach that we present generalizes in a straightforward manner to higher order controlled gates, such as CCCX gates, which are useful in quantum error correction, where parity measurements using this method could also be executed. These higher order gates could also be useful for quantum simulators of high energy physics or quantum chemistry simulators where three-body interactions are crucial for emulating interactions between gauge and matter fields.

See the [supplementary material](#) for detail of the derivation of the circuit Hamiltonian and explicit expressions of neglected perturbations and higher order accumulated phases.

This work has received funding from the European Union's Horizon 2020 research and innovation program under Grant Agreement No. 828826 "Quomorphic" and the MSCA Cofund Action under No. 847471 "Qustec," from the German Federal Ministry of Education and Research via the funding program quantum technologies—from basic research to the market under Contract No. 13N15684 and 13N15680 "GeQCoS," and support from EPSRC DTP under Grant No. EP/R513040/1.

AUTHOR DECLARATIONS

Conflict of Interest

All authors declare that they have no conflicts of interest.

DATA AVAILABILITY

Data sharing is not applicable to this article as no new data were created or analyzed in this study.

REFERENCES

1. F. Arute, K. Arya, R. Babbush *et al.*, "Quantum supremacy using a programmable superconducting processor," *Nature* **574**(7779), 505–510 (2019).
2. J. Preskill, "Quantum computing in the NISQ era and beyond," *Quantum* **2**, 79 (2018).
3. V. V. Shende and I. L. Markov, "On the CNOT-cost of TOFFOLI gates," *Quantum Info. Comput.* **9**(5), 461–486 (2009).
4. P. W. Shor, "Scheme for reducing decoherence in quantum computer memory," *Phys. Rev. A* **52**, R2493–R2496 (1995).
5. L. K. Grover, "A fast quantum mechanical algorithm for database search," *Assoc. Comput. Mach. in Proceedings of the 28th Annual ACM Symposium on Theory of Computing* (ACM, 1996), pp. 212–219.
6. Y. Cao, J. Romero, J. P. Olson *et al.*, "Quantum chemistry in the age of quantum computing," *Chem. Rev.* **119**(19), 10856–10915 (2019).
7. S. McArdle, S. Endo, A. Aspuru-Guzik, S. C. Benjamin, and X. Yuan, "Quantum computational chemistry," *Rev. Mod. Phys.* **92**, 015003 (2020).
8. S. E. Rasmussen, K. Groenland, R. Gerritsma, K. Schoutens, and N. T. Zinner, "Single-step implementation of high-fidelity n -bit Toffoli gates," *Phys. Rev. A* **101**, 022308 (2020).
9. X. Xu and M. H. Ansari, "ZZ freedom in two-qubit gates," *Phys. Rev. Appl.* **15**, 064074 (2021).
10. M. C. Collodo, A. Potočník, S. Gasparinetti *et al.*, "Observation of the crossover from photon ordering to delocalization in tunably coupled resonators," *Phys. Rev. Lett.* **122**, 183601 (2019).
11. Y. Sung, L. Ding, J. Braumüller *et al.*, "Realization of high-fidelity CZ and ZZ-free iSWAP gates with a tunable coupler," *Phys. Rev. X* **11**, 021058 (2021).
12. M. Khazali and K. Mølmer, "Fast multiqubit gates by adiabatic evolution in interacting excited-state manifolds of Rydberg atoms and superconducting circuits," *Phys. Rev. X* **10**, 021054 (2020).
13. Y. Wu, W.-S. Bao, S. Cao *et al.*, "Strong quantum computational advantage using a superconducting quantum processor," *Phys. Rev. Lett.* **127**, 180501 (2021).
14. A. Fedorov, L. Steffen, M. Baur, M. P. Da Silva, and A. Wallraff, "Implementation of a Toffoli gate with superconducting circuits," *Nature* **481**(7380), 170–172 (2012).
15. A. D. Hill, M. J. Hodson, N. Didier, and M. J. Reagor, "Realization of arbitrary doubly-controlled quantum phase gates," *arXiv:2108.01652* [quant-ph] (2021).
16. Y. Kim, A. Morvan, L. B. Nguyen *et al.*, "High-fidelity iToffoli gate for fixed-frequency superconducting qubits," *arXiv:2108.10288* [quant-ph] (2021).
17. M. C. Collodo, J. Herrmann, N. Lacroix *et al.*, "Implementation of conditional phase gates based on tunable ZZ interactions," *Phys. Rev. Lett.* **125**, 240502 (2020).
18. P. Jurcevic, A. Javadi-Abhari, L. S. Bishop *et al.*, "Demonstration of quantum volume 64 on a superconducting quantum computing system," *Quantum Sci. Technol.* **6**(2), 025020 (2021).
19. E. A. Sete, A. Q. Chen, R. Manenti, S. Kulshreshtha, and S. Poletto, "Floating tunable coupler for scalable quantum computing architectures," *Phys. Rev. Appl.* **15**, 064063 (2021).
20. S. E. Nigg and S. M. Girvin, "Stabilizer quantum error correction toolbox for superconducting qubits," *Phys. Rev. Lett.* **110**, 243604 (2013).
21. B. Royer, S. Puri, and A. Blais, "Qubit parity measurement by parametric driving in circuit QED," *Sci. Adv.* **4**(11), 1695 (2018).
22. M. Sameti and M. J. Hartmann, "Floquet engineering in superconducting circuits: From arbitrary spin–spin interactions to the Kitaev honeycomb model," *Phys. Rev. A* **99**, 012333 (2019).
23. J. Jin, D. Rossini, R. Fazio, M. Leib, and M. J. Hartmann, "Photon solid phases in driven arrays of nonlinearly coupled cavities," *Phys. Rev. Lett.* **110**, 163605 (2013).
24. Y. Chen, C. Neill, P. Roushan *et al.*, "Qubit architecture with high coherence and fast tunable coupling," *Phys. Rev. Lett.* **113**, 220502 (2014).
25. F. Yan, P. Krantz, Y. Sung *et al.*, "Tunable coupling scheme for implementing high-fidelity two-qubit gates," *Phys. Rev. Appl.* **10**, 054062 (2018).
26. X. Li, T. Cai, H. Yan *et al.*, "Tunable coupler for realizing a controlled-phase gate with dynamically decoupled regime in a superconducting circuit," *Phys. Rev. Appl.* **14**, 024070 (2020).
27. J. M. Chow, A. D. Córcoles, J. M. Gambetta *et al.*, "Simple all-microwave entangling gate for fixed-frequency superconducting qubits," *Phys. Rev. Lett.* **107**, 080502 (2011).

- ²⁸J. Majer, J. M. Chow, J. M. Gambetta *et al.*, “Coupling superconducting qubits via a cavity bus,” *Nature* **449**(7161), 443–447 (2007).
- ²⁹J. Koch, T. M. Yu, J. Gambetta *et al.*, “Charge-insensitive qubit design derived from the Cooper pair box,” *Phys. Rev. A* **76**, 042319 (2007).
- ³⁰S. Bravyi, D. P. DiVincenzo, and D. Loss, “Schrieffer–Wolff transformation for quantum many-body systems,” *Ann. Phys.* **326**(10), 2793–2826 (2011).
- ³¹G. Zhu, D. G. Ferguson, V. E. Manucharyan, and J. Koch, “Circuit QED with fluxonium qubits: Theory of the dispersive regime,” *Phys. Rev. B* **87**, 024510 (2013).
- ³²R. Cleve and D. P. DiVincenzo, “Schumacher’s quantum data compression as a quantum computation,” *Phys. Rev. A* **54**, 2636–2650 (1996).
- ³³J. R. Johansson, P. D. Nation, and F. Nori, “Qutip: An open-source Python framework for the dynamics of open quantum systems,” *Comput. Phys. Commun.* **183**(8), 1760–1772 (2012).
- ³⁴N. Wittler, F. Roy, K. Pack *et al.*, “Integrated tool set for control, calibration, and characterization of quantum devices applied to superconducting qubits,” *Phys. Rev. Appl.* **15**, 034080 (2021).
- ³⁵F. Motzoi, J. M. Gambetta, P. Rebentrost, and F. K. Wilhelm, “Simple pulses for elimination of leakage in weakly nonlinear qubits,” *Phys. Rev. Lett.* **103**, 110501 (2009).
- ³⁶D. C. McKay, S. Filipp, A. Mezzacapo *et al.*, “Universal gate for fixed-frequency qubits via a tunable bus,” *Phys. Rev. Appl.* **6**, 064007 (2016).
- ³⁷M. Sameti, A. Potočnik, D. E. Browne, A. Wallraff, and M. J. Hartmann, “Superconducting quantum simulator for topological order and the Toric code,” *Phys. Rev. A* **95**, 042330 (2017).
- ³⁸M. A. Nielsen and I. L. Chuang, *Quantum Computation and Quantum Information: 10th Anniversary Edition*, 10th ed. (Cambridge University Press, 2011).
- ³⁹A. Barenco, C. H. Bennett, R. Cleve *et al.*, “Elementary gates for quantum computation,” *Phys. Rev. A* **52**, 3457–3467 (1995).
- ⁴⁰A. M. Steane, “Error correcting codes in quantum theory,” *Phys. Rev. Lett.* **77**, 793–797 (1996).
- ⁴¹N. Chancellor, S. Zohren, and P. A. Warburton, “Circuit design for multi-body interactions in superconducting quantum annealing systems with applications to a scalable architecture,” *npj Quantum Inf.* **3**(1), 1–6 (2017).